# Further Shortening of the C−C Single Bond in Substituted Tetrahedranyl Tetrahedrane Systems: An Energy Decomposition Analysis†

**Gaddamanugu Gayatri,‡ Yarasi Soujanya,‡ Israel Fernández,§ Gernot Frenking,*,§ and G. Narahari Sastry*,‡**

*Indian Institute of Chemical Technology, Hyderabad-500 607, India, and Fachbereich Chemie, Philipps-Universität Marburg, Hans-Meerwein-Strasse, D-35043 Marburg, Germany*

*Received: April 3, 2008; Revised Manuscript Received: April 20, 2008*

The computational study explores the electronic fine tuning of the exocyclic C−C single bond length in tetrahedranyl tetrahedrane as a function of various substituents. The factors which determine the bond lengths and bond strengths are examined by using the EDA method.

## Introduction

Bond lengths and bond strengths are fundamental parameters in chemistry. It is generally assumed that bond lengths and bond strengths, which are given by the bond dissociation energy (BDE), are inversely related to each other. However, such a correlation is not always given, and there are many cases known where a longer bond may be stronger than a shorter bond between the same atoms.[1] A recent analysis of the nature of the covalent bond showed that it is the exchange (Pauli) repulsion between electrons which have the same spin that determines the equilibrium distance of a covalent bond rather than the overlap of the atomic orbitals.[2] The rather delicate balance between attractive forces arising from the interactions between not completely filled orbital (covalent bonding) and the repulsive forces arising from the interactions between filled orbital (Pauli repulsion) leads to equilibrium structures which are minima on the potential energy surface. A third contribution to the energy comes from the Coulombic interactions between the atoms which is in most cases strongly attractive, even for most neutral molecules.[2]

A typical C−C single bond has an equilibrium distance of around 1.54 Å, but sometimes, chemists encounter unusually long or unusually short bonds. The factors responsible for such a stretching and shrinking of the bonds and their consequences on bond strengths provide a major impetus and challenge for theoretical studies. It is known that in case of cage compounds, the ring strain is associated with the shortening of the bond in both exoskeletal and skeletal bonds.[3] Recent work of Tanaka and Sekiguchi on the structure of trimethyl-silyl substituted tetrahedranyl tetrahedrane (**THTH**) reports the shortest acyclic C−C single bond of 1.426 Å. The shortening was traced to the high s character at the carbon orbitals forming the exocyclic bond.[4] These observations are in agreement with earlier theoretical predictions.[3] The experimental results further triggered incisive theoretical probes to delineate the causative reasons for such a shortening, which suggested that hyperconjugation may play a major role in bond shortening.[5]

According to the energy decomposition analysis (EDA) which was employed by two of the current authors,[6] the C−C bond strength in **THTH** is higher by about 30% compared to ethane and much higher compared to substituted analogues of ethane. In contrast, the central C−C linkage in the bicubyl system, which held the record for the shortest C−C bond prior to the synthesis of substituted **THTH**, was found to be not particularly stronger compared to ethane, albeit it is much shorter. Thus, the **THTH** represents not only the shortest but arguably the strongest C−C single bond known. According to the EDA results, the stronger and shorter C−C bond in the **THTH** system compared with the bicubyl compound does not come from more attractive interactions but from much less Pauli repulsion between the tetrahedryl moieties.[6] This finding clearly indicates that bond shortening and bond strengthening may be caused by factors that can only be brought to light by a thorough bonding analysis which considers all aspects of the interatomic interactions. We want to point out that the effects of electron-withdrawing and electron-donating substituents on cyclic and acyclic systems have also been studied by other groups.[7–13]

This work aims to delineate the effects of various substituents, H, $CH_3$, OH, OMe, $NH_2$, $SiH_3$, F, Cl, Br, and CN, given in Figure 1, on the exoskeletal C−C single bond. Furthermore, the relative stability of eclipsed and staggered conformations in these substituted systems is examined. Finally, a correlation between the exocyclic C−C single bond length and its bond strength, by using EDA method, is explained. EDA method involves contributions from the various interactions and thus has been used to carry out a detailed analysis of such interactions for the present set of systems. Natural bond orbital (NBO) calculations were carried out to examine the hybridization of the linking exoskeletal carbons.

## Methods

Geometry optimizations for all compounds were first carried out by using gradient corrected DFT, B3LYP level[14] in conjunction with 6-311+G(d,p) basis sets. The calculations were done with the program package Gaussian03.[15] All structures are characterized as minima or saddle points on the potential energy surface by calculating the vibrational frequencies. The hybridization at the carbon atoms in the exocyclic C−C bond was estimated with the NBO method.[16] The nature of the exocyclic C−C bond was analyzed by means of the EDA scheme of ADF[17] which was originally

† Part of the "Sason S. Shaik Festschrift".

* To whom correspondence should be addressed. (G. F.) Phone: +49-(0)6421-2825563. Fax: +49(0)6421-2825566. E-mail: frenking@chemie.uni-marburg.de and (G. N. S.) Phone: +91-40-27160123. Fax: +91-40-27160512. E-mail: gnsastry@gmail.com.

‡ Indian Institute of Chemical Technology.

§ Philipps-Universität Marburg.

10.1021/jp802886g CCC: $40.75 
Published on Web 06/13/2008

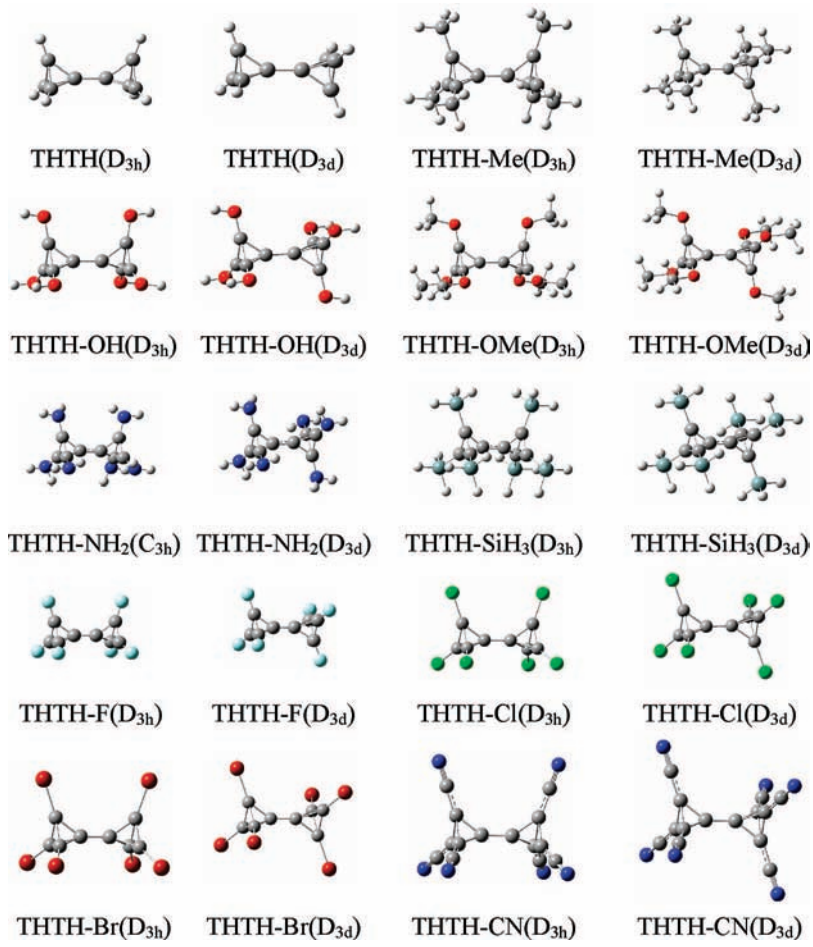


**Figure 1.** Structures and symmetry of the energy minima of the **THTH**−X compounds ($D_{3d}$) and the transition states ($D_{3h}$ or $C_{3h}$) investigated in this work.

developed by Morokuma[18] and by Ziegler and Rauk.[19] The focus of the bonding analysis is the instantaneous interaction energy, $\Delta E_{int}$, of the bond, which is the energy difference between the **THTH** molecule and the tetrahedranyl fragments at the electronic doublet state in the frozen geometry of the compound. The interaction energy can be divided into three main components:

$$\Delta E_{int} = \Delta E_{elstat} + \Delta E_{Pauli} + \Delta E_{orb} \quad (1)$$

$\Delta E_{elstat}$ gives the electrostatic interaction energy between the fragments and the molecule, which is calculated by using the frozen electron density distribution of the interacting species. The second term in eq 1, $\Delta E_{Pauli}$, refers to the repulsive interactions between the fragments, which are caused by the fact that two electrons with the same spin cannot occupy the same region in space. $\Delta E_{Pauli}$ is calculated by enforcing the Kohn−Sham determinant on the superimposed fragments to obey the Pauli principle by antisymmetrization and renormalization. The stabilizing orbital interaction term, $\Delta E_{orb}$ is calculated in the final step of the energy partitioning analysis when the Kohn−Sham orbitals relax to their optimal form. This term can be further partitioned into contributions by the orbitals belonging to different irreducible representations of the point group of the interacting system. The interaction energy, $\Delta E_{int}$, can be used to calculate the BDE, $D_e$, by adding $\Delta E_{prep}$, which is the energy necessary to promote the fragments from their equilibrium geometry to the geometry in the compounds (eq 2). Further details of the energy partitioning analysis can be found in the literature.[17b]

$$-D_e = \Delta E_{prep} + \Delta E_{int} \quad (2)$$

The EDA calculations have been carried out at the BP86[20] level by using uncontracted Slater-type basis functions which have TZ2P quality.[21] An auxiliary set of s, p, d, f, g, and h Slater-type orbitals was used to fit the molecular densities and to represent the Coulomb and exchange potentials accurately in each self-consistent field cycle.[22] For the EDA calculations, the geometries were optimized at BP86/TZ2P.

## Results and Discussion

Table 1 gives the exocyclic C−C single bond lengths, hybridization of the carbons linking the exoskeletal bond, and the barriers for rotation about the C−C bond, which were calculated at B3LYP/6-311+G(d,p). Table 2 lists the EDA results for the staggered conformers at BP86/TZ2P. Careful examination of the calculated numbers gives insights into the factors which determine the bond length and the bond strength. Although the changes in the exocyclic C−C distances are small, the analysis of the calculated numbers reveal important information about the theoretically predicted trends.

From the comparison of eclipsed and staggered conformations of substituted **THTH** systems, it can be observed from Table 1 that the eclipsed conformations possess longer exoskeletal C−C bonds than the staggered conformations. This cannot be ascribed to a higher s character of the carbon atoms linking the exocyclic

**TABLE 1: Bond Lengths for the Exocyclic C−C Bond in Angstroms, NImag Values, and Hybridization (Hyb$^n$) for the Eclipsed and Staggered Conformations and Rotational Barriers (RB) at B3LYP/6-311+G(d,p) Level**

| | eclipsed | | | staggered | | | |
|---|---|---|---|---|---|---|---|
| name | bond length | NImag | Hyb$^n$ | bond length | NImag | Hyb$^n$ | RB |
| **THTH** | 1.435 | 1 | $sp^{1.48}$ | 1.426 | 0 | $sp^{1.46}$ | 2.8 |
| **THTH**−Me | 1.436 | 1 | $sp^{1.46}$ | 1.428 | 0 | $sp^{1.45}$ | 2.2 |
| **THTH**−OH | 1.432 | 3[a] | $sp^{1.39}$ | 1.424 | 0 | $sp^{1.38}$ | 2.1 |
| **THTH**−OMe | 1.431 | 1 | $sp^{1.39}$ | 1.424 | 0 | $sp^{1.40}$ | 2.3 |
| **THTH**−$NH_2$ | 1.436 | 1 | $sp^{1.43}$ | 1.428 | 0 | $sp^{1.43}$ | 4.0 |
| **THTH**−$SiH_3$ | 1.433 | 1 | $sp^{1.53}$ | 1.427 | 0 | $sp^{1.53}$ | 2.4 |
| **THTH**−F | 1.423 | 3[a] | $sp^{1.29}$ | 1.415 | 0 | $sp^{1.28}$ | 2.3 |
| **THTH**−Cl | 1.421 | 1 | $sp^{1.40}$ | 1.415 | 0 | $sp^{1.40}$ | 2.1 |
| **THTH**−Br | 1.421 | 1 | $sp^{1.44}$ | 1.414 | 0 | $sp^{1.43}$ | 2.2 |
| **THTH**−CN | 1.427 | 1 | $sp^{1.42}$ | 1.420 | 0 | $sp^{1.42}$ | 1.9 |

[a] One of the frequencies corresponds to the exocyclic C−C single bond rotation. The other two have very small absolute values and are likely the results of numerical integral calculations.

bonds of the staggered conformations. The NBO values for the hybridization change very little upon rotation, and the s character of the C−C bonds in the staggered conformation is sometimes slightly higher but sometimes slightly lower than that in the eclipsed conformation. The data clearly show that there must be other factors than the change in the hybridization which determine the length of the C−C bond. On the other hand, the calculated hybridization indicates that the C−C bond orbitals have a very large s character between $sp^{1.28}$−$sp^{1.53}$, which is clearly much higher than in a $sp^3$ hybridized orbital. The data suggest that the hybridization plays a major role for the very short C−C bonds in the **THTH** systems. We want to point out that the calculated energy difference between the staggered equilibrium form and the eclipsed saddle point of **THTH** is in very good agreement with a previous study where the staggered conformation was found to be more stable than the eclipsed conformation by 2.8 kcal/mol.[5]

The calculated values at B3LYP/6-311+G(d,p) for the exoskeletal C−C bond of the staggered equilibrium structures show that the substituted **THTH**s may be divided into two groups. One group are the halogen-substituted systems **THTH**−X, where X = F, Cl, or Br. These three compounds have nearly the same exocyclic C−C distance of 1.414−1.415 Å (Table 1), which is clearly shorter than in the parent compound (1.426 Å). If they could be synthesized, they would exhibit the shortest C−C single bond which has ever been observed. The members of the other group of **THTH**−X, where X = Me, OH, OMe, $NH_2$, or $SiH_3$, have essentially the same exoskeletal C−C distance (1.424−1.428 Å) as in the parent molecule. The exocyclic C−C distance of the compound **THTH**−CN, which has a pseudo-halogen as substituent, has an intermediate value (1.420 Å). It is gratifying that the calculated values at BP86/TZ2P give very similar values and that the above grouping holds also for the latter data. The only exception is the C−C distance where X = $NH_2$, for which the BP86/TZ2P value (1.417 Å) is shorter than that at B3LYP/6-311+G(d,p) (1.428 Å).

We will now discuss the EDA results given in Table 2 in order to rationalize the changes in the exoskeletal C−C distances. First, we notice that there is no correlation between the bond length and the bond strength of the C−C bond. This holds if one takes the intrinsic interaction energy $\Delta E_{int}$ or the BDE $D_e$ as measure for the bond strength. For example, the compound **THTH**−Br has a significantly shorter bond than the parent system, but the BDE ($D_e$ = 133.8 kcal/mol) is less than that for **THTH** ($D_e$ = 136.2 kcal/mol), and also the $\Delta E_{int}$ value of the former (−141.3 kcal/mol) is slightly less than that for the latter (−142.6 kcal/mol). A similar situation is found when one compares the exocyclic C−C distances and the bond strength of **THTH**−CN with the parent system **THTH**. In the following, we will use the intrinsic interaction energy $\Delta E_{int}$ as measure for the bond strength because the BDE comprises also the preparation energy $\Delta E_{prep}$, which is not directly related to the interatomic interactions. We want to point out that the trend of $\Delta E_{int}$ and $D_e$ is the same for all compounds. This is because the $\Delta E_{prep}$ do not vary a lot.

A pivotal question concerns the strength of the hyperconjugation in **THTH**−X. Table 2 shows that the stabilization gained by the $\pi$ orbitals contributes between 12.1 and 15.0% to the total orbital interactions. A previous work showed that the $\pi$-orbital interactions in substituted unconstrained ethanes $X_3C-CX_3$ provide between 5.4 (X = H) and 10.0% (X = Cl) to the $\Delta E_{orb}$ term.[6] Although the C−C bonds in **THTH**−X are significantly shorter than those in $X_3C-CX_3$, the increase in the stabilizing contribution of the $\pi$-orbital interactions is rather small. This is a first hint that hyperconjugation may not be the main driving force for the short C−C bond.

Table 2 shows that **THTH**−Me has a longer and weaker exocyclic C−C bond than **THTH**. However, the contributions of the electrostatic attraction $\Delta E_{elstat}$ and the orbital interactions $\Delta E_{orb}$ in **THTH**−Me are significantly stronger than those in **THTH**. Note that the increase in $\Delta E_{orb}$ comes mainly from the $\sigma$ orbitals, whereas the hyperconjugation, which is given by the $\pi$ orbitals, increases only slightly. The increase of the attractive terms is compensated by the larger Pauli repulsion. Thus, the longer and weaker exoskeletal C−C bond in **THTH**−Me comes from the stronger steric repulsion of the methyl substituents, which is in agreement with chemical intuition. The EDA data for **THTH**−OH show that the exocyclic C−C bond is also weaker than that in **THTH**, but now, the bond length of the former system is slightly shorter than that in the parent system. The electrostatic attraction $\Delta E_{elstat}$ in **THTH**−OH has nearly the same strength as that in **THTH**, whereas the orbital interactions $\Delta E_{orb}$ in the former compound are clearly stronger than those in the latter. Note that the contribution of the $\pi$ orbitals to the larger $\Delta E_{orb}$ value has increased from 12.1% in **THTH** to 13.0% in **THTH**−OH (Table 2). There is stronger hyperconjugation in the latter system than in the parent compound, which agrees with the notion that electronegative substituents yield lower-lying vacant orbitals which are available for hyperconjugation. The stronger hyperconjugation can be correlated to the slightly shorter exocyclic C−C bond in **THTH**−OH than that in

**TABLE 2: EDA Results at BP86/TZ2P for the Exocyclic C−C Bond of Staggered THTH−X at the Equilibrium Geometry[a]**

| | H | Me | OH | OMe | $NH_2$ | $SiH_3$ | F | Cl | Br | CN |
|---|---|---|---|---|---|---|---|---|---|---|
| $\Delta E_{int}$ | −142.6 | −138.8 | −139.9 | −139.8 | −127.9 | −137.3 | −144.9 | −141.7 | −141.3 | −136.0 |
| $\Delta E_{Pauli}$ | 225.2 | 244.9 | 237.0 | 243.2 | 333.2 | 259.2 | 233.1 | 286.3 | 303.2 | 285.1 |
| $\Delta E_{elstat}$ | −144.0 (39.2%) | −153.5 (40.0%) | −144.7 (38.2%) | −146.4 (38.2%) | −185.3 (40.2%) | −159.7 (39.5%) | −136.8 (36.2%) | −166.3 (38.8%) | −173.9 (39.1%) | −154.2 (36.6%) |
| $\Delta E_{Orb}$ | −223.8 (60.8%) | −230.2 (60.0%) | −232.2 (61.6%) | −236.5 (61.8%) | −275.8 (59.8%) | −239.8 (60.5%) | −241.2 (63.8%) | −261.7 (61.2%) | −270.7 (60.9%) | −266.9 (63.4%) |
| $\Delta E_{\sigma}$ $(a_1)^b$ | −196.7 (87.9%) | −202.1 (87.8%) | −202.0 (87.0%) | −205.9 (87.1%) | −240.8 (87.4%) | −210.4 (87.8%) | −205.6 (85.2%) | −224.0 (85.6%) | −232.4 (85.9%) | −226.6 (84.9%) |
| $\Delta E_{\delta}$ $(a_2)^b$ | <−0.1 | −0.1 | <−0.1 | <−0.1 | −0.1 | <−0.1 | <−0.1 | <−0.1 | <−0.1 | −0.1 |
| $\Delta E_{\pi}$ $(e)^b$ | −27.1 (12.1%) | −28.0 (12.2%) | −30.2 (13.0%) | −30.5 (12.9%) | −34.9 (12.6%) | −29.3 (12.2%) | −35.6 (14.8%) | −37.6 (14.4%) | −38.2 (14.1%) | −40.2 (15.0%) |
| $\Delta E_{prep}$ | 6.4 | 6.9 | 6.7 | 7.4 | 6.5 | 7.6 | 6.6 | 7.4 | 7.5 | 8.4 |
| $\Delta E$ $(= -D_e)$ | −136.2 | −131.9 | −133.2 | −132.4 | −121.4 | −129.7 | −138.3 | −134.3 | −133.8 | −127.6 |
| $r(C-C)_{exo}$ | 1.426 | 1.431 | 1.422 | 1.424 | 1.417 | 1.426 | 1.413 | 1.410 | 1.410 | 1.418 |
| $S(C-C)_{exo}$ | 0.486 | 0.465 | 0.476 | 0.466 | 0.373 | 0.439 | 0.481 | 0.424 | 0.404 | 0.410 |

[a] The interacting species are the tetrahedryl fragments in the electronic doublet state. Energy values are in kcal/mol, and distances are in Angstroms. The last line gives the size of the overlap of the atomic orbitals $S$ between the carbon atoms in the exocyclic C−C bond. [b] The fragments have $C_{3v}$ symmetry which gives orbital contributions with $a_1$, $a_2$, and $e$ symmetry.

**TABLE 3: EDA Results at BP86/TZ2P for the Exocyclic C−C Bond of Staggered THTH−X Calculated at the Frozen Bond Length $r(C-C)_{exo}$ = 1.426 Å[a]**

| | H | Me | OH | OMe | $NH_2$ | $SiH_3$ | F | Cl | Br | CN |
|---|---|---|---|---|---|---|---|---|---|---|
| $\Delta E_{int}$ | −142.6 | −138.9 | −139.9 | −139.6 | −127.8 | −137.3 | −144.7 | −141.5 | −141.1 | −135.9 |
| $\Delta E_{Pauli}$ | 225.2 | 248.1 | 234.2 | 241.7 | 325.7 | 259.2 | 224.2 | 274.2 | 290.2 | 278.8 |
| $\Delta E_{elstat}$ | −144.0 (39.2%) | −155.1 (40.1%) | −143.4 (38.3%) | −145.7 (38.2%) | −181.7 (40.1%) | −159.7 (39.5%) | −132.9 (36.0%) | −160.6 (38.6%) | −167.8 (38.9%) | −151.3 (36.5%) |
| $\Delta E_{Orb}$ | −223.8 (60.8%) | −231.9 (59.9%) | −230.7 (61.7%) | −235.6 (61.8%) | −271.8 (59.9%) | −239.8 (60.5%) | −236.0 (64.0%) | −255.1 (61.4%) | −263.6 (61.1%) | −263.4 (63.5%) |
| $\Delta E_{\sigma}$ $(a_1)^b$ | −196.7 (87.9%) | −203.2 (87.7%) | −201.0 (87.1%) | −205.3 (87.2%) | −238.0 (87.6%) | −210.4 (87.8%) | −202.2 (85.7%) | −219.6 (86.1%) | −227.6 (86.4%) | −224.2 (85.1%) |
| $\Delta E_{\delta}$ $(a_2)^b$ | <−0.1 | −0.1 | <−0.1 | <−0.1 | −0.1 | <−0.1 | <−0.1 | <−0.1 | <−0.1 | −0.1 |
| $\Delta E_{\pi}$ $(e)^b$ | −27.1 (12.1%) | −28.5 (12.3%) | −29.7 (12.9%) | −30.2 (12.8%) | −33.7 (12.4%) | −29.3 (12.2%) | −33.8 (14.3%) | −35.5 (13.9%) | −36.0 (13.6%) | −39.0 (14.8%) |
| $\Delta E_{prep}$ | 6.4 | 6.9 | 6.8 | 7.2 | 6.5 | 7.6 | 6.5 | 7.4 | 7.4 | 8.4 |
| $\Delta E$ $(= -D_e)$ | −136.2 | −132.0 | −133.1 | −132.4 | −121.3 | −129.7 | −138.2 | −134.1 | −133.7 | −127.5 |

[a] The interacting species are the tetrahedryl fragments in the electronic doublet state. Energy values are in kcal/mol. [b] The fragments have $C_{3v}$ symmetry which gives orbital contributions with $a_1$, $a_2$, and $e$ symmetry.

**THTH**, but they do not yield a stronger bond. The EDA data show that the larger Pauli repulsion in the former compound compensates for the increase in the attractive terms. The EDA results for **THTH**−OMe are very similar to those of **THTH**−OH (Table 2). The exocyclic C−C bond distance and the bond strength in the two compounds are nearly the same. The slightly larger values for $\Delta E_{elstat}$ and $\Delta E_{orb}$ in **THTH**−OMe are compensated by an equally strong increase of the Pauli repulsion, which can be explained with the larger steric repulsion of the OMe substituents compared with OH.

The amino-substituted system **THTH**−$NH_2$ has clearly the weakest exoskeletal C−C bond ($\Delta E_{int} = -127.9$ kcal/mol) of all compounds investigated here, but the bond distance of 1.417 Å is even shorter than that in **THTH** (1.426 Å). Note that the strength of the attractive components $\Delta E_{elstat}$ and $\Delta E_{orb}$ in **THTH**−$NH_2$ are the largest of all systems shown in Table 2. This is a surprising result considering the fact that the C−C interaction energy $\Delta E_{int}$ is rather small. The large contributions of the attractive terms are overcompensated by the large Pauli repulsion. Table 2 shows that **THTH**−$NH_2$ has also the largest $\Delta E_{Pauli}$ value, which can be explained with the repulsion of the nitrogen lone-pair orbitals which are more diffuse than the oxygen lone-pair orbitals and thus yield stronger exchange repulsion. We want to point out that the hyperconjugation in **THTH**−$NH_2$ (−34.9 kcal/mol) is clearly higher than that in **THTH**−OH (−30.5 kcal/mol), but the main increase of the $\Delta E_{orb}$ term comes from the $\sigma$ orbitals. The EDA results for the silyl-substituted system **THTH**−$SiH_3$ are similar to those of **THTH**−Me. The Pauli repulsion in the former system is slightly stronger than that in the latter because the $SiH_3$ substituent is more bulky than $CH_3$, but the attractive terms $\Delta E_{elstat}$ and $\Delta E_{orb}$ in **THTH**-$SiH_3$ are also a bit stronger, which nearly compensates for the larger steric repulsion.

The halogen-substituted systems **THTH**−X (X = F, Cl, Br) have clearly the shortest exocyclic C−C bonds (Table 2), but the bond strengths given by the $\Delta E_{int}$ values are similar to the C−C bond strength in the parent system **THTH**. The Pauli repulsion in **THTH**−X significantly increases with F < Cl < Br, which can be explained with the size of the halogen atoms. The rise in the repulsive forces is nearly compensated by the stronger attraction, which comes from the orbital interactions and Coulombic interactions alike. The rise is particulalry steep from fluorine to chlorine, which can be explained with the more diffuse orbital at the carbon atoms of the exocyclic C−C bond which leads to better overlaps and stronger attraction with the carbon nucleus of the adjacent carbon atom. Table 1 shows that the $sp^n$ hybridization of the carbon atoms change toward more p character with the trend F < Cl < Br. We want to point out that the contribution of the $\pi$ orbitals to $\Delta E_{orb}$ is very high, which indicates a rather strong hyperconjugation. The largest contribution of hyperconjugation to the exoskeletal C−C bond is calculated for **THTH**−CN (Table 2). Although the C−C bond in the latter compound is rather short, it is the second weakest after the amino-substituted species **THTH**−$NH_2$. This comes from a comparatively large Pauli repulsion which compensates for the intrinsically strong orbital attraction and Coulombic attraction. It has been shown by us that the maximum in the stabilizing interactions is not determined by the size of the overlap of the atomic orbital but by the steep increase of the Pauli repulsion at shorter interatomic distances. The attractive orbital interactions and electrostatic bonding further increase when a bond becomes shorter than the equilibrium value but $\Delta E_{Pauli}$ becomes much larger.[9]

Table 2 shows also the overlap integrals of the singly occupied fragment orbitals which yield the exocyclic C−C bonds. A surprising result is the very small value $S = 0.373$ for **THTH**−$NH_2$, because the molecule has the strongest orbital interaction ($\Delta E_{orb} = -275.8$ kcal/mol) of all systems shown in Table 2. Equally surprising is the largest value $S = 0.486$ which is found for the parent system **THTH**−H, because it has the weakest orbital interaction ($\Delta E_{orb} = -223.8$ kcal/mol). It has been shown before that the size of the overlap does not correlate with the strength of a bond.[2]

The EDA results in Table 2 have been obtained by using the equilibrium structures of the tetrahedrane systems. It is interesting to compare the data with EDA results for **THTH**−X where the exocyclic C−C bond is frozen at the distance of the parent system **THTH**−H (1.426 Å). The EDA results for the latter species where all geometry variables have been optimized except for the frozen C−C bond are shown in Table 3.

The values given in Table 3 show that the overall interaction energies $\Delta E_{int}$ at $r$(C−C) = 1.426 Å do not differ very much from the equilibrium values (Table 2), whereas the energy components exhibit a somewhat larger variation. It is enlightening to analyze the trend of the energy terms for the different systems shown in Table 3, because the size depends only on the type of ligand but not on the geometry. The following trends are observed:

$$\Delta E_{Pauli}: F < H < OH < OMe < Me < SiH_3 < Cl < CN < Br < < NH_2$$

$$\Delta E_{elstat}: F < OH < H < OMe < CN < Me < SiH_3 < Cl < Br < NH_2$$

$$\Delta E_{Orb}: H < OH < Me < OMe < F < SiH_3 < Cl < CN < Br < NH_2$$

Noteworthy is the finding than the amino-substituted system has the largest values for all three energy terms, particularly for the Pauli repulsion which is much larger than that in the next member of the series, Br. This is clearly the effect of the diffuse lone-pair orbital at nitrogen. It is surprising, however, that the amino group yields also the strongest electrostatic attraction and the strongest orbital term. As shown above, this is not due to the larger orbital overlap of the carbon atoms which make up the exocyclic C−C bond.

## Summary and Conclusion

The results of the present work can be summarized as follows. The very short exocyclic C−C single bond in **THTH**−X can be further shortened when X is a halogen atom. The calculations predict that the C−C bond will become shorter by ~0.012 Å when X = F, Cl, Br compared to that in the silyl-subsituted compound **THTH**−$SiH_3$. The EDA results reveal that the equilibrium bond length of the exocyclic C−C single bond is determined by the interplay of attractive forces (electrostatic bonding and orbital interactions) and repulsive forces (Pauli repulsion), where it is the latter which prevents shorter bonds. Although the hyperconjugation in **THTH**−X is slightly stronger than that in substituted ethanes $X_3C-CX_3$, the main reason for the very short exoskeletal C−C single bond in the former compound is the very high s character of the bonding orbital at carbon.

**Acknowledgment.** G.G. thanks CSIR, India, for the research fellowship. This work was supported by the Deutsche Forschungsgemeinschaft. G.N.S. thanks DST for the Swarnajayanthi grant.

**Supporting Information Available:** This material is available free of charge via the Internet at http://pubs.acs.org.

## References and Notes

(1) (a) Frenking, G.; Wichmann, K.; Fröhlich, N.; Grobe, J.; Golla, W.; Le Van, D.; Krebs, B.; Läge, M. *Organometallics* **2002**, *21*, 2921. (b) Uddin, J.; Frenking, G. *J. Am. Chem. Soc.* **2001**, *123*, 1683. (c) Frenking, G.; Wichmann, K.; Fröhlich, N.; Loschen, C.; Lein, M.; Frunzke, J.; Rayón, V. M. *Coord. Chem. Rev.* **2003**, *238*−*239*, 55. (d) LeinM., FrenkingG. In *Theory and Applications of Computational Chemistry: The First 40 Years*; Dykstra, C. E., Frenking, G., Kim, K. S., ScuseriaG.E., Eds.; Elsevier: Amsterdam, 2005; p 367.

(2) Krapp, A.; Bickelhaupt, F. M.; Frenking, G. *Chem. Eur. J.* **2006**, *12*, 9196.

(3) (a) Xie, Y.; Schaefer, H. F., III *Chem. Phys. Lett.* **1989**, *161*, 516. (b) Xie, Y.; Schaefer, H. F., III *Chem. Phys. Lett.* **1990**, *168*, 249.

(4) Tanaka, M.; Sekiguchi, A. *Angew. Chem., Int. Ed.* **2005**, *44*, 5821.

(5) Mo, Y. *Org. Lett.* **2006**, *8*, 535.

(6) Fernandez, I.; Frenking, G. *Chem. Eur. J.* **2006**, *12*, 3617.

(7) Mo, Y.; Lin, Z. *J. Chem. Phys.* **1996**, *105*, 1046.

(8) Clark, T.; Spitznagel, G. W.; Klose, R.; Schleyer, P. v. R. *J. Am. Chem. Soc.* **1984**, *106*, 4412.

(9) Durmaz, S.; Kollmar, H. *J. Am. Chem. Soc.* **1980**, *102*, 6942.

(10) Cremer, D.; Kraka, E. *J. Am. Chem. Soc.* **1985**, *107*, 3811.

(11) Dill, J. S.; Greenberg, A.; Liebman, J. F. *J. Am. Chem. Soc.* **1979**, *101*, 6814.

(12) Demachy, I.; Volatron, F. *J. Phys. Chem.* **1994**, *98*, 10728.

(13) Mo, Y.; Jiao, H.; Schleyer, P. v. R. *J. Org. Chem.* **2004**, *69*, 3493.

(14) (a) Becke, A. D. *J. Chem. Phys.* **1993**, *98*, 5648. (b) Lee, C.; Yang, W.; Parr, R. G. *Phys. Rev. B* **1988**, *37*, 785. (c) Stevens, P. J.; Devlin, F. J.; Chablowski, C. F.; Frisch, M. J. *J. Phys. Chem.* **1994**, *98*, 11623.

(15) Frisch, M. J.; Trucks, G. W.; Schlegel, H. B.; Scuseria, G. E.; Robb, M. A.; Cheeseman, J. R.; Montgomery, J. A., Jr.; Vreven, T.; Kudin, K. N.; Burant, J. C.; Millam, J. M.; Iyengar, S. S.; Tomasi, J.; Barone, V.; Mennucci, B.; Cossi, M.; Scalmani, G.; Rega, N.; Petersson, G. A.; Nakatsuji, H.; Hada, M.; Ehara, M.; Toyota, K.; Fukuda, R.; Hasegawa, J.; Ishida, M.; Nakajima, T.; Honda, Y.; Kitao, O.; Nakai, H.; Klene, M.; Li, X.; Knox, J. E.; Hratchian, H. P.; Cross, J. B.; Bakken, V.; Adamo, C.; Jaramillo, J.; Gomperts, R.; Stratmann, R. E.; Yazyev, O.; Austin, A. J.; Cammi, R.; Pomelli, C.; Ochterski, J. W.; Ayala, P. Y.; Morokuma, K.; Voth, G. A.; Salvador, P.; Dannenberg, J. J.; Zakrzewski, V. G.; Dapprich, S.; Daniels, A. D.; Strain, M. C.; Farkas, O.; Malick, D. K.; Rabuck, A. D.; Raghavachari, K.; Foresman, J. B.; Ortiz, J. V.; Cui, Q.; Baboul, A. G.; Clifford, S.; Cioslowski, J.; Stefanov, B. B.; Liu, G.; Liashenko, A.; Piskorz, P.; Komaromi, I.; Martin, R. L.; Fox, D. J.; Keith, T.; Al-Laham, M. A.; Peng, C. Y.; Nanayakkara, A.; Challacombe, M.; Gill, P. M. W.; Johnson, B.; Chen, W.; Wong, M. W.; Gonzalez, C.; Pople, J. A. *Gaussian 03*, revision C.02; Gaussian, Inc.: Wallingford, CT, 2004.

(16) Reed, A. E.; Curtiss, L. A.; Weinhold, F. *Chem. Rev.* **1988**, *88*, 899.

(17) (a) Bickelhaupt, F. M.; Baerends, E. J. In *Rev. Comput. Chem.*; Lipkowitz, K.B., BoydD.B., Eds.; Wiley-VCH: New York, 2000; Vol. 15, p 1. (b) te Velde, G.; Bickelhaupt, F. M; Baerends, E. J.; van Gisbergen, S. J. A.; Fonseca Guerra, C.; Snijders, J. G.; Ziegler, T. *J. Comput. Chem.* **2001**, *22*, 931.

(18) Morokuma, K. J. *Chem. Phys.* **1971**, *55*, 1236.

(19) Ziegler, T.; Rauk, A. *Theor. Chim. Acta* **1977**, *46*, 1.

(20) (a) Becke, A. D. *Phys. Rev. A* **1988**, *38*, 3098. (b) Perdew, J. P. *Phys. Rev. B* **1986**, *33*, 8822.

(21) Snijders, J. G.; Baerends, E. J.; Vernooijs, P. *At. Nucl. Data Tables* **1982**, *26*, 483.

(22) Krijn, J.; Baerends, E. J. Fit Functions in the HFS-Method. *Internal Report (in Dutch)*; Vrije Universiteit Amsterdam: The Netherlands, 1984.

JP802886G